Transcriptomic study of probenecid on injured spinal cords in mice

Yu-Xin Zhang Equal first author, 1, 2, 3 , **Sai-Nan Wang** Equal first author, 1, 2 , **Jing Chen** 1, 2 , **Jian-Guo Hu** Corresp., 1, 2 , **He-Zuo Lü** Corresp. 1, 2

1 Clinical Laboratory, the First Affiliated Hospital of Bengbu Medical College, Bengbu, China

2 Anhui Key Laboratory of Tissue Transplantation, the First Affiliated Hospital of Bengbu Medical College, Bengbu, China

3 Department of Biochemistry and Molecular Biology, Bengbu Medical College, Bengbu, China

Corresponding Authors: Jian-Guo Hu, He-Zuo Lü
Email address: jghu9200@163.com, lhz233003@163.com

Background . Recent studies have found that probenecid has neuroprotective and repairing roles for central nervous system (CNS) injury. However, its effect on genome-wide transcription in acute spinal cord injury (SCI) remains unknown. Therefore, in the present study, RNA sequencing (RNA-Seq) was used to analyze the effect of probenecid on the local expression of gene transcription 8 h following injury. **Methods.** An Infinite Horizon impactor was used to perform contusive SCI in mice. The SCI model was made by using a rod (1.3 mm diameter) with a force of 50 Kdynes. Sham-operated (sham) mice only received a laminectomy without contusive injury. The spinal cord injured mice were randomly assigned into the control (SCI_C) or probenecid injection (SCI_P) group. The drug was intraperitoneal injected (0.5mg/kg, intraperitoneally) immediately following injury. Eight hours after operation, the spinal cords were removed. The total RNAs were extracted and purified for library preparation and transcriptomesequencing. Differential gene expressions (DEGs) of three groups were analyzed using the DESeq. Gene Ontology (GO) and Kyoto Encyclopedia of Genes and Genomes (KEGG) enrichment analysis of DEGs were performed using GOseq R package and KOBAS. Real-time quantitative reverse-transcriptase polymerase chain reaction (RT-qPCR) was used to validate RNA-Seq results. **Results.** RNA-Seq showed that, as compared with the SCI_C group, the number of DEGs was 641 in the SCI_P group (286 upregulated and 355 downregulated). According to GO analysis, DEGs were most enriched in extracellular matrix, collagen trimer, protein bounding and sequence specific DNA binding. KEGG analysis showed that the most enriched pathways included Cell adhesion molecules (CAMs), Leukocyte transendothelial migration, ECM-receptor interaction, PI3K-Akt signaling pathway, Hematopoietic cell lineage, Focal adhesion, Rap1 signaling pathway, etc. The sequence data have been deposited into Sequence Read Archive (https://www.ncbi.nlm.nih.gov/sra/PRJNA554464).

Transcriptomic study of probenecid on injured spinal cords in mice

Yu-Xin Zhang[1,2,3&], Sai-Nan Wang[1,2&], Jing Chen[1,2], Jian-Guo Hu[1,2*], He-Zuo Lü[1, 2*]

[1] Clinical Laboratory, the First Affiliated Hospital of Bengbu Medical College, Anhui 233004, P.R. China

[2]Anhui Key Laboratory of Tissue Transplantation, the First Affiliated Hospital of Bengbu Medical College, Anhui 233004, P.R. China

[3]Department of Biochemistry and Molecular Biology, Bengbu Medical College, Anhui 233030, P.R. China

& These authors contributed equally to this work

* Co-corresponding authors:

Jian-Guo Hu

Email address: jghu9200@163.com

He-Zuo Lü

Email address: lhz233003@163.com

Please address correspondence to:

He-Zuo Lü, M.D. Ph.D., Professor

Anhui Key Laboratory of Tissue Transplantation

the First Affiliated Hospital of Bengbu Medical College

287 Chang Huai Road

Bengbu 233004, P.R. China

Tel: +86-552-3170692

E-mail: lhz233003@163.com

Abstract

Background. Recent studies have found that probenecid has neuroprotective and repairing roles for central nervous system (CNS) injury. However, its effect on genome-wide transcription in acute spinal cord injury (SCI) remains unknown. Therefore, in the present study, RNA sequencing (RNA-Seq) was used to analyze the effect of probenecid on the local expression of gene transcription 8 h following injury.
Methods. An Infinite Horizon impactor was used to perform contusive SCI in mice. The SCI model was made by using a rod (1.3 mm diameter) with a force of 50 Kdynes. Sham-operated (sham) mice only received a laminectomy without contusive injury. The spinal cord injured mice were randomly assigned into the control (SCI_C) or probenecid injection (SCI_P) group. The drug was intraperitoneal injected (0.5mg/kg, intraperitoneally) immediately following injury. Eight hours after operation, the spinal cords were removed. The total RNAs were extracted and purified for library preparation and transcriptome sequencing. Differential gene expressions (DEGs) of three groups were analyzed using the DESeq. Gene Ontology (GO) and Kyoto Encyclopedia of Genes and Genomes (KEGG) enrichment analysis of DEGs were performed using GOseq R package and KOBAS. Real-time quantitative reverse-transcriptase polymerase chain reaction (RT-qPCR) was used to validate RNA-Seq results.
Results. RNA-Seq showed that, as compared with the SCI_C group, the number of DEGs was 641 in the SCI_P group (286 upregulated and 355 downregulated). According to GO analysis, DEGs were most enriched in extracellular matrix, collagen trimer, protein bounding and sequence specific DNA binding. KEGG analysis showed that the most enriched pathways included Cell adhesion molecules (CAMs), Leukocyte transendothelial migration, ECM-receptor interaction, PI3K-Akt signaling pathway, Hematopoietic cell lineage, Focal adhesion, Rap1 signaling pathway, etc. The sequence data have been deposited into Sequence Read Archive (https://www.ncbi.nlm.nih.gov/sra/PRJNA554464).

Introduction

Spinal cord injury (SCI) is defined as a variety of injuries to the spinal cord. According to the severity of injury, the symptoms may vary, ranging from pain to complete loss of movement and sensory function. SCI affects millions of people worldwide and usually affects patients for life (Friedli et al. 2015). In the United States, the incidence of SCI ranges from 12,000 to 20,000 cases a year, with more than 280,000 patients sitting in wheelchairs (Singh et al. 2014). In the past decade, the SCI cases in China have increased tenfold, and now 60,000 cases are increased every year (Qiu 2009). SCI has a high rate of disability and mortality, which brings heavy burden to patients, families and society (Krueger et al. 2013). Therefore, it is self-evident to explore the effective treatment methods for repairing SCI in order to improve the quality of life of patients and reduce the burden of social medical care.
According to the different stages, the pathological processes following traumatic SCI can be divided into primary injury and secondary injury (Geisler et al. 2002; McDonald & Sadowsky 2002). Primary injury refers to the direct injury of the spinal cord by mechanical force, including compression, contusion, laceration and penetration. Secondary injury refers to edema, ischemia, local inflammation and electrolyte changes. These changes can cause accumulation of lipid peroxides and oxygen free radicals, release of inflammatory factors and proteases, and lead to a large number of cell apoptosis or necrosis, which further aggravates the damage of neurons and axons (Ahuja et al. 2017; Oyinbo 2011; Tran et al. 2018).

Probenecid is an organic anion transport protein inhibitor, which has been widely used in clinic (Hagos et al. 2017; Tollner et al. 2015). For example, probenecid has been used as a synergist in the treatment of gout and antibiotics (Baranova et al. 2004; Papadopoulos & Verkman 2008). It can reduce the degree of cognitive impairment in rats with cognitive impairment (Mawhinney et al. 2011). It can also reverse cerebral ischemic injury and cellular inflammation (Wei et al. 2015; Xiong et al. 2014). The combination of probenecid and N-Acetylcysteine could produce additive effects by maintaining intracellular GSH concentrations and inhibiting neuronal death after traumatic stretch injury (Du et al. 2016). Some studies had reported that probenecid can also reduce neuropathic pain in the spinal cord (Bravo et al. 2014; Pineda-Farias et al. 2013). Therefore, these reports indicate that probenecid has neuroprotective and repairing roles for central nervous system (CNS) injury. However, whether the drug can play a role in SCI and whether it can affect the gene expression profiles in injured spinal cords remain unknown. Therefore, in the present study, probenecid was injected intraperitoneally into spinal cord injured mice immediately after injury. Eight hours after operation, the spinal cords were removed, and RNA-Seq was used to analyze the changes of transcriptome expression in the injured area, then the key molecules and signal pathways were screened and identified, and provided new theoretical and experimental basis for SCI clinical treatment.

Materials & Methods

Animals

A total of 27 healthy and clean C57BL/6 female mice (18-20g, 8 weeks old) were used to model SCI. The animal care and use committee of Bengbu Medical College provided full approval for this research (037/2017). Animal care following surgery was in compliance with the regulations for the management of experimental animals (revised by the Ministry of Science and Technology of China in June 2004), as well as the guidelines and policies on rodent survival surgery provided by the Animal Care and Use Committee of Bengbu Medical College.

Contusive SCI and drug injection

An Infinite Horizon impactor (Precision Systems & Instrumentation, Lexington, KY) was used to perform contusive SCI. The mice were firstly anesthetized with 50 mg/kg pentobarbitally, then the T9 lamina was excised, the SCI model was created using a rod (1.3 mm diameter) with a force of 50 Kdynes. Sham-operated (sham) mice only received a laminectomy without contusive injury.

The spinal cord injured mice were randomly assigned to the solvent control (SCI_C) or probenecid injection (SCI_P) group. The solvent or probenecid (0.5mg/kg) was intraperitoneally injection immediately following injury. The solution (pH 7.3) was prepared as previously described (Hainz et al. 2017).

RNA isolation, quantification and qualification

Eight hours after operation, the mice were anesthetized and perfused with 10 ml PBS, and then the spinal cords (0.5 cm including the injury center) were removed. The total RNAs from spinal cords were extracted and purified as previously described (Shi et al. 2017).

Library preparation and transcriptome sequencing

The sequencing libraries were produced by using NEBNext® Ultra™ RNA Library Prep Kit for Illumina® (NEB, USA) as previously described (Shi et al. 2017). Finally, the 125 bp/150 bp paired-end reads were obtained and sequenced on an Illumina Hiseq platform.

Analysis of differentially expressed gene (DEG)

Prior to DEG analysis,, the gene expression statistics were analyzed by using RSEM software (http://deweylab.biostat.wisc.edu/rsem/) to convert the read count numbers to Fragments Per Kilobase of transcript per Million fragments mapped (FPKM), and Principal Component Analysis (PCA) analysis was made to determine the similarity and difference of data. DEGs of three groups were analyzed as previously described (Shi et al. 2017) by using the DESeq software (http://www.bioconductor.org/). Benjamini and Hochberg's approach was used to control the false discovery rate and adjust the P-values. The adjusted P-value < 0.05 was defined as a standard for significant differences in gene expression. In addition to FPKM hierarchical clustering analysis of DEGs, we further analyzed the subclusters based on log2 (ratios) of the gene expression level relative to that of sham group. The log2 (ratios) in SCI_C group ≥ 1 or ≤ -1 was used as a cut-off for subcluster analysis. The clustering algorithm divided the DEGs which have similar expression trends into several subclusters.

Gene Ontology (GO) and Kyoto Encyclopedia of Genes and Genomes (KEGG) enrichment analysis of DEGs

The GO and KEGG analysis were performed by using GOseq R package and KOBAS software as previously described (Shi et al. 2017). In GO analysis, DEGs were implemented by the GOseq R package, in which gene length bias was corrected. GO terms with corrected P value ≤ 0.05 were considered significantly enriched by DEGs. KEGG is a database resource for understanding high-level functions and utilities of the biological system (http://www.genome.jp/kegg/). In this study, we used KOBAS software to test the statistical enrichment of DEGs in KEGG pathways.

Real-time quantitative reverse-transcriptase polymerase chain reaction (RT-qPCR)

To validate RNA-Seq results, 9 DEGs were randomly selected and verified by RT-qPCR according to our previous methods (Shi et al. 2017). The analysis was performed in 6 samples, which included 3 independent samples and the 3 same samples used for the RNA-seq analysis. PCR primer sequences are listed in Table 1. The relative quantitative results of each group of genes were calculated according to the formula of $^{\Delta\Delta}$Ct (Livak & Schmittgen 2001). The statistical values (n=6/group) were presented as mean ± standard deviation (SD). The data were analyzed using one-way ANOVA followed by Student–Newman–Keuls tests. Statistical differences were considered significant at P < 0.05.

Results

Identification of expressed transcripts the mice spinal cords

For the quality assessment of sequencing data, nine cDNA libraries were established, including sham (sham_1, sham_2 and sham_3), SCI_C (SCI_C1, SCI_C2 and SCI_C3) and SCI_P (SCI_P1, SCI_P2 and SCI_P3). RNA-Seq produced 48,848,744 - 61,037,096 raw reads for each sample. After filtering out the low-quality reads, the clean reads were 48,226,002 - 60,037,772, with the Q30 (%) 93.67 - 94.31 (Table 2).

In order to identify the source of variation in the original data, PCA analysis was conducted. As shown in Fig.1, PC1, PC2 and PC3 were 54.51, 12.33 and 7.09%, respectively. The distance between SCI_C (or SCI_P) and sham was obvious. Although the distance between SCI_P and sham is not too far, it is sufficient for the analysis. These demonstrated that the data could be used for the next analysis.

Effect of SCI and probenecid treatment on gene expression

RPKM and DEGSeq were used to analyze the gene expression level and differential expression profiles, respectively. The results showed that, as compared with the sham group, there were 4,617 DEGs inthe SCI_C group, including 2,904 upregulated and 1,713 downregulated genes

(Fig.2A and Table S1). As compared with the SCI_C group, there were 641 different genes in the SCI_P group, 286 were upregulated and 355 were downregulated (Fig.2B and Table S1). The sequence data have been deposited into Sequence Read Archive (https://www.ncbi.nlm.nih.gov/sra/PRJNA554464).

RT-qPCR identification of DEGs

In order to verify the RNA-Seq results, nine DEGs were randomly selected from the SCI_P group, as compared with the SCI_C group, namely Itga1, Lamb1, Cldn5, Lama2, CD34, Esam, Setdb2, Agrn and Ccnt2. The RNA-Seq and RT-qPCR results indicated that the expression patterns of these DEGs were similar (Fig.3).

Cluster Analysis of DEGs

The DEGs from different groups were analyzed using FPKM hierarchical cluster analysis. As shown in Fig. 4, DEGs were classified into different expression clusters by hierarchical clustering. These clusters contained upregulated or downregulated DEGs. Most upregulated DEGs in the SCI_C group as compared with the sham group, were in the middle and upper clusters, while downregulated DEGs were observed in the lower cluster. As compared with the sham group, most upregulated DEGs in the SCI_P group were in the upper cluster, while downregulated DEGs were mainly observed in the lower cluster. As compared withthe SCI_C group, some upregulated DEGs in the SCI_P group were observed in upper cluster, while downregulated DEGs were observed in the middle cluster; there were also some clusters with no significant differences.

In addition to FPKM hierarchical clustering analysis of DEGs, the subclusters which have similar expression trends were further analyzed. The log2 (ratios) in SCI_C group ≥ 1 or ≤ -1 was used as a cut-off for subcluster analysis. As shown in Fig. 5, we found several subclusters with similar expression trends. Based on log2 (ratios) of the gene expression level relative to that of sham group, the log2 (ratios) of all gene expression levels in sham group were zero. Fig. 5 A and B showed that the two subclusters were strongly upregulated following SCI, and then downregulated upon probenecid treatment. Fig. 5 C and D showed that the two subclusters were strongly downregulated following SCI, and then upregulated upon probenecid treatment. In Fig. 5A, six genes (Cybb, Esam, Itgam, Itgb2, Msn and Ncf2) were involved in the leukocyte transendothelial migration signaling pathway; six genes (Col4a1, Erbb2, Flt4, Nos3, Syk and Thbs4) were involved in the PI3K-Akt signaling pathway. In Fig. 5B, three genes (Cyba, Ncf1 and Rac2) were involved in the NADPH oxidases; two genes (Cflar and Tnfrsf10b) were involved in the TRAIL signaling pathway; eight genes (Cd63, Cyba, Ddx58, Fcer1g, Lyn, Myh9, Ncf1 and Psmb8) were involved in the innate immune system. In Fig. 5C and D, no gene can be clustered into valuable signaling pathways.

Go enrichment analysis of DEGs

As compared with the sham group, there were seventy-eight GO terms in upregulated DEGs (Fig.6A, Table S2) and nine GO terms in downregulated DEGs (Fig.6B, Table S2) in the SCI_C group. The upregulated DEGs were most enriched in binding, protein binding, chemokine activity, chemokine receptor binding, G-protein coupled receptor binding, anion binding, small GTPase mediated signal transduction, immune system process, immune response, etc. The downregulated DEGs were most enriched in protein binding, binding, extracellular-glutamate-gated ion channel activity, acid phosphatase activity, transporter activity, mannose metabolic process, excitatory extracellular ligand-gated ion channel activity, transmembrane transporter activity, anion transmembrane and transporter activity. In SCI_P group, we observed three GO terms in downregulated DEGs (Fig.6C, Table S3) and no valuable terms in upregulated DEGs

(Table S3) as compared with the SCI_C group. The downregulated DEGs were protein binding, binding and sequence-specific DNA binding.

KEGG enrichment analysis of DEGs

Scatter plot were used to express the KEGG enrichment analysis results for the DEGs. As compared with the sham group, the upregulated DEGs in the SCI_C group were most enriched in TNF, NF-kappa B, cytokine-cytokine receptor interaction, Toll-like receptor, Leukocyte transendothelial migration, PI3K-Akt, Focal adhesion, apoptosis, etc. (Fig.7A, Table S4); the downregulated DEGs were most enriched in glutamatergic synapse, basal cell carcinoma, axon guidance, other glycan degradation and nicotine addiction (Fig.7B, Table S4). In the SCI_P group vs SCI_C group, only "ECM-receptor interaction" was enriched in the upregulated DEGs (Fig.7C, Table S5); the downregulated DEGs were enriched in cell adhesion molecules (CAMs), malaria, leukocyte transendothelial migration, ECM-receptor interaction, PI3K-Akt signaling pathway, hematopoietic cell lineage, focal adhesion, Rap1 signaling pathway and amoebiasis (Fig.7D, Table S5).

Discussion

Recent studies have shown that probenecid has neuroprotective and repairing effects in the process of brain disorders (Wei et al. 2015; Xiong et al. 2014). However, its effect on genome-wide transcription in acute spinal cord injury (SCI) is still unknown. Therefore, in this study, RNA-Seq was used to analyze the effect of probenecid on the local expression of gene transcription eight hours after SCI. The results showed that, as compared with the sham group, there were 4,617 DEGs in the SCI_C group, including 2,904 upregulated and 1,713 downregulated genes. As compared with the SCI_C group, there were 641 DEGs in the SCI_P group, 286 were upregulated and 355 were downregulated. These are consistent with others and our previous reports (Chen et al. 2013; Shi et al. 2017). It also shows that the results of this experiment are reliable. As compared with the SCI_C, there were 641 DEGs in theSCI_P group, 286 were upregulated and 355 were downregulated. To further verify the RNA-seq results, we randomly selected 9 DEGs (Itga1, Lamb1, Cldn5, Lama2, CD34, Esam, Setdb2, Agrn and Ccnt2) for RT-qPCR. The results showed that the expression patterns of these genes detected by these two methods were similar, indicating that our RNA-seq results are reliable and can be used for subsequent analysis. These also confirmed that probenecid can alter gene transcription after SCI.

In order to further analyze the DEGs effected by probenecid, we used GO enrichment which can reflect the distribution of DEGs on GO term enriched in cell components, molecular functions and biological processes (Huang et al. 2013). In the SCI_P vs SCI_C group, the analysis showed that there were 3 GO terms in downregulated DEGs (protein binding, binding and sequence-specific DNA binding) and no valuable terms in upregulated DEGs. KEGG analysis showed that the valuable signaling pathways associated with these DEGs included CAMs, leukocyte transendothelial migration, ECM-receptor interaction, PI3K-Akt signaling pathway, hematopoietic cell lineage, focal adhesion, Rap1 signaling pathway, etc.

Among these signal pathways, some have been reported to be related to SCI, such as CAMs (Brook et al. 2000; Zhang et al. 2008), ECM-receptor interaction (Zhou et al. 2017), PI3K-Akt signaling pathway (Li et al. 2019a; Li et al. 2019b; Zhang et al. 2017) and focal adhesion (Chuang et al. 2018; Graham et al. 2016; Hao et al. 2018).

Following SCI, probenecid treatment could downregulate some genes, subclusters and signaling pathways. Leukocyte transendothelial migration from the blood into tissues is vital for immune

surveillance and inflammation (Cook-Mills 2006).There is a large amount of leukocyte infiltration in the pathological process of SCI. The infiltration of leukocytes need bind to endothelial cell adhesion molecules and then migrate between vascular endothelial cells (Wang et al. 2011). Therefore, the inhibition of leukocyte transendothelial migration and CAMs induced by probenecid may play a role in inhibiting inflammation by weakening the infiltration of white blood cells in the injured area. In this study, we clustered six genes (Cybb, Esam, Itgam, Itgb2, Msn and Ncf2) involved in this pathway. Their expression is strongly downregulated following SCI, and then upregulated upon probenecid treatment. This just proves that probenecid treatment following SCI can play an anti-inflammatory role by inhibiting the infiltration of inflammatory cells.

The ECM plays an important role in tissue and organ morphogenesis (Bonnans et al. 2014; Rabelink et al. 2017) and control of cellular activities such as adhesion, migration, differentiation, proliferation and apoptosis (Yue 2014). Focal adhesions are specialized intracellular sites in which aggregated integrin receptors interact with extracellular matrices, while extracellular matrices interact with intracellular actin cytoskeleton (Burridge 2017; LaFlamme et al. 2018). At the same time, focal adhesions are the result of cell-extracellular matrix (ECM) interactions (Burridge 2017; De Pascalis & Etienne-Manneville 2017). ECM and Focal adhesions are downregulated after probenecid treatment, indicating that probenecid might improve SCI by inhibiting adhesion, migration, differentiation, proliferation and apoptosis.

It has been reported that PI3K-Akt signaling fuses a variety of extracellular and intracellular signal transduction pathways that regulate macrophage biology, including the production of pro-inflammatory cytokines, phagocytosis, autophagy and homeostasis (Vergadi et al. 2017). PI3K-Akt signal pathway is downregulated in SCI after probenecid treatment, and there are six genes (Col4a1, Erbb2, Flt4, Nos3, Syk and Thbs4) being clustered into this pathway, indicating that probenecid might improve SCI by regulating macrophages and inhibiting inflammatory pathways. This is likely to provide important clues into the mechanism of action of probenecid. The relationship between hematopoietic cell lineage pathway and SCI was found in a report on the bioinformatics analysis of SCI (Zhu et al. 2017). Its specific role has not been reported yet, and deserves further discussion.

Rap1 signal pathway plays an important role in regulating cell-cell and cell-matrix interactions by regulating the function of adhesion molecules (Kim et al. 2011; Pollan et al. 2018). In our study, Rap1 signaling pathway was enriched in downregulated DEGs of SCI after probenecid treatment, suggesting that probenecid may inhibit cell adhesion and polarization by inhibiting the Rap1 signaling pathway, thereby inhibiting inflammation.

In addition, three genes (Cyba, Ncf1 and Rac2) related to the NADPH oxidases, two genes (Cflar and Tnfrsf10b) related to the TRAIL signaling pathway and eight genes (Cd63, Cyba, Ddx58, Fcer1g, Lyn, Myh9, Ncf1 and Psmb8) related to the innate immune system were also strongly downregulated following probenecid treatment. We know that NADPH oxidases is involved in oxidative stress, TRALL signaling pathway mediates inflammation and apoptosis, and the immune system is involved in almost all pathological processes of injury (Chyuan et al. 2018; Ewald 2018; Tisato et al. 2018). Therefore, probenecid treatment can play a neuroprotective role by inhibiting immune response, oxidative stress, anti-inflammation and anti-apoptosis after SCI.

Conclusions

Acute SCI can lead to changes of mRNAs in injured spinal cords. These mRNAs and their related pathways could provide some explanations for the pathological mechanism of acute SCI. More interestingly, we also demonstrated that probenecid can lead to gene expression inhibitions

in the acute injured spinal cord. These downregulated DEGs and their associated signaling pathways, such as focal adhesion, leukocyte transendothelial migration, ECM-receptor interaction, PI3K-Akt, Rap1, are mainly related to inflammatory response, local hypoxia, macrophage differentiation, adhesion migration and apoptosis of local cells. This suggests that the application of probenecid in acute phase can improve the local microenvironment of SCI. However, whether probenecid can be used as a therapeutic drug for SCI still needs to be further explored. Next, the detailed research on this subject will be conducted by combining animal models and clinical practice.

References

Ahuja CS, Nori S, Tetreault L, Wilson J, Kwon B, Harrop J, Choi D, and Fehlings MG. 2017. Traumatic Spinal Cord Injury-Repair and Regeneration. *Neurosurgery* 80:S9-S22. 10.1093/neuros/nyw080

Baranova A, Ivanov D, Petrash N, Pestova A, Skoblov M, Kelmanson I, Shagin D, Nazarenko S, Geraymovych E, Litvin O, Tiunova A, Born TL, Usman N, Staroverov D, Lukyanov S, and Panchin Y. 2004. The mammalian pannexin family is homologous to the invertebrate innexin gap junction proteins. *Genomics* 83:706-716. 10.1016/j.ygeno.2003.09.025

Bonnans C, Chou J, and Werb Z. 2014. Remodelling the extracellular matrix in development and disease. *Nat Rev Mol Cell Biol* 15:786-801. 10.1038/nrm3904

Bravo D, Ibarra P, Retamal J, Pelissier T, Laurido C, Hernandez A, and Constandil L. 2014. Pannexin 1: a novel participant in neuropathic pain signaling in the rat spinal cord. *Pain* 155:2108-2115. 10.1016/j.pain.2014.07.024

Brook GA, Houweling DA, Gieling RG, Hermanns T, Joosten EA, Bar DP, Gispen WH, Schmitt AB, Leprince P, Noth J, and Nacimiento W. 2000. Attempted endogenous tissue repair following experimental spinal cord injury in the rat: involvement of cell adhesion molecules L1 and NCAM? *Eur J Neurosci* 12:3224-3238.

Burridge K. 2017. Focal adhesions: a personal perspective on a half century of progress. *FEBS J* 284:3355-3361. 10.1111/febs.14195

Chen K, Deng S, Lu H, Zheng Y, Yang G, Kim D, Cao Q, and Wu JQ. 2013. RNA-seq characterization of spinal cord injury transcriptome in acute/subacute phases: a resource for understanding the pathology at the systems level. *PLoS One* 8:e72567. 10.1371/journal.pone.0072567

Chuang YC, Lee CH, Sun WH, and Chen CC. 2018. Involvement of advillin in somatosensory neuron subtype-specific axon regeneration and neuropathic pain. *Proc Natl Acad Sci U S A* 115:E8557-E8566. 10.1073/pnas.1716470115

Chyuan IT, Tsai HF, Wu CS, Sung CC, and Hsu PN. 2018. TRAIL-Mediated Suppression of T Cell Receptor Signaling Inhibits T Cell Activation and Inflammation in Experimental Autoimmune Encephalomyelitis. *Front Immunol* 9:15. 10.3389/fimmu.2018.00015

Cook-Mills JM. 2006. Hydrogen peroxide activation of endothelial cell-associated MMPs during VCAM-1-dependent leukocyte migration. *Cell Mol Biol (Noisy-le-grand)* 52:8-16.

De Pascalis C, and Etienne-Manneville S. 2017. Single and collective cell migration: the mechanics of adhesions. *Mol Biol Cell* 28:1833-1846. 10.1091/mbc.E17-03-0134

Du L, Empey PE, Ji J, Chao H, Kochanek PM, Bayir H, and Clark RS. 2016. Probenecid and N-Acetylcysteine Prevent Loss of Intracellular Glutathione and Inhibit Neuronal Death after Mechanical Stretch Injury In Vitro. *J Neurotrauma* 33:1913-1917. 10.1089/neu.2015.4342

354 Ewald CY. 2018. Redox Signaling of NADPH Oxidases Regulates Oxidative Stress Responses,
355 Immunity and Aging. *Antioxidants (Basel)* 7. 10.3390/antiox7100130
356 Friedli L, Rosenzweig ES, Barraud Q, Schubert M, Dominici N, Awai L, Nielson JL, Musienko
357 P, Nout-Lomas Y, Zhong H, Zdunowski S, Roy RR, Strand SC, van den Brand R, Havton
358 LA, Beattie MS, Bresnahan JC, Bezard E, Bloch J, Edgerton VR, Ferguson AR, Curt A,
359 Tuszynski MH, and Courtine G. 2015. Pronounced species divergence in corticospinal tract
360 reorganization and functional recovery after lateralized spinal cord injury favors primates.
361 *Sci Transl Med* 7:302ra134. 10.1126/scitranslmed.aac5811
362 Geisler FH, Coleman WP, Benzel E, Ducker T, and Hurlbert RJ. 2002. Spinal cord injury. *Lancet*
363 360:1883; author reply 1884. 10.1016/s0140-6736(02)11744-2
364 Graham ZA, Qin W, Harlow LC, Ross NH, Bauman WA, Gallagher PM, and Cardozo CP. 2016.
365 Focal adhesion kinase signaling is decreased 56 days following spinal cord injury in rat
366 gastrocnemius. *Spinal Cord* 54:502-509. 10.1038/sc.2015.183
367 Hagos FT, Daood MJ, Ocque JA, Nolin TD, Bayir H, Poloyac SM, Kochanek PM, Clark RS, and
368 Empey PE. 2017. Probenecid, an organic anion transporter 1 and 3 inhibitor, increases
369 plasma and brain exposure of N-acetylcysteine. *Xenobiotica* 47:346-353.
370 10.1080/00498254.2016.1187777
371 Hainz N, Wolf S, Beck A, Wagenpfeil S, Tschernig T, and Meier C. 2017. Probenecid arrests the
372 progression of pronounced clinical symptoms in a mouse model of multiple sclerosis. *Sci*
373 *Rep* 7:17214. 10.1038/s41598-017-17517-5
374 Hao M, Ji XR, Chen H, Zhang W, Zhang LC, Zhang LH, Tang PF, and Lu N. 2018. Cell cycle and
375 complement inhibitors may be specific for treatment of spinal cord injury in aged and
376 young mice: Transcriptomic analyses. *Neural Regen Res* 13:518-527. 10.4103/1673-
377 5374.226405
378 Huang Q, Wu LY, Wang Y, and Zhang XS. 2013. GOMA: functional enrichment analysis tool
379 based on GO modules. *Chin J Cancer* 32:195-204. 10.5732/cjc.012.10151
380 Kim C, Ye F, and Ginsberg MH. 2011. Regulation of integrin activation. *Annu Rev Cell Dev Biol*
381 27:321-345. 10.1146/annurev-cellbio-100109-104104
382 Krueger H, Noonan VK, Trenaman LM, Joshi P, and Rivers CS. 2013. The economic burden of
383 traumatic spinal cord injury in Canada. *Chronic Dis Inj Can* 33:113-122.
384 LaFlamme SE, Mathew-Steiner S, Singh N, Colello-Borges D, and Nieves B. 2018. Integrin and
385 microtubule crosstalk in the regulation of cellular processes. *Cell Mol Life Sci* 75:4177-
386 4185. 10.1007/s00018-018-2913-x
387 Li H, Zhang X, Qi X, Zhu X, and Cheng L. 2019a. Icariin Inhibits Endoplasmic Reticulum Stress-
388 induced Neuronal Apoptosis after Spinal Cord Injury through Modulating the PI3K/AKT
389 Signaling Pathway. *Int J Biol Sci* 15:277-286. 10.7150/ijbs.30348
390 Li Y, Guo Y, Fan Y, Tian H, Li K, and Mei X. 2019b. Melatonin Enhances Autophagy and
391 Reduces Apoptosis to Promote Locomotor Recovery in Spinal Cord Injury via the
392 PI3K/AKT/mTOR Signaling Pathway. *Neurochem Res* 44:2007-2019. 10.1007/s11064-
393 019-02838-w
394 Livak KJ, and Schmittgen TD. 2001. Analysis of relative gene expression data using real-time
395 quantitative PCR and the 2(-Delta Delta C(T)) Method. *Methods* 25:402-408.
396 10.1006/meth.2001.1262
397 Mawhinney LJ, de Rivero Vaccari JP, Dale GA, Keane RW, and Bramlett HM. 2011. Heightened
398 inflammasome activation is linked to age-related cognitive impairment in Fischer 344 rats.
399 *BMC Neurosci* 12:123. 10.1186/1471-2202-12-123

McDonald JW, and Sadowsky C. 2002. Spinal-cord injury. *Lancet* 359:417-425. 10.1016/S0140-6736(02)07603-1

Oyinbo CA. 2011. Secondary injury mechanisms in traumatic spinal cord injury: a nugget of this multiply cascade. *Acta Neurobiol Exp (Wars)* 71:281-299.

Papadopoulos MC, and Verkman AS. 2008. Potential utility of aquaporin modulators for therapy of brain disorders. *Prog Brain Res* 170:589-601. 10.1016/S0079-6123(08)00446-9

Pineda-Farias JB, Perez-Severiano F, Gonzalez-Esquivel DF, Barragan-Iglesias P, Bravo-Hernandez M, Cervantes-Duran C, Aguilera P, Rios C, and Granados-Soto V. 2013. The L-kynurenine-probenecid combination reduces neuropathic pain in rats. *Eur J Pain* 17:1365-1373. 10.1002/j.1532-2149.2013.00305.x

Pollan SG, Huang F, Sperger JM, Lang JM, Morrissey C, Cress AE, Chu CY, Bhowmick NA, You S, Freeman MR, Spassov DS, Moasser MM, Carter WG, Satapathy SR, Shah K, and Knudsen BS. 2018. Regulation of inside-out beta1-integrin activation by CDCP1. *Oncogene* 37:2817-2836. 10.1038/s41388-018-0142-2

Qiu J. 2009. China Spinal Cord Injury Network: changes from within. *Lancet Neurol* 8:606-607. 10.1016/S1474-4422(09)70162-0

Rabelink TJ, van den Berg BM, Garsen M, Wang G, Elkin M, and van der Vlag J. 2017. Heparanase: roles in cell survival, extracellular matrix remodelling and the development of kidney disease. *Nat Rev Nephrol* 13:201-212. 10.1038/nrneph.2017.6

Shi LL, Zhang N, Xie XM, Chen YJ, Wang R, Shen L, Zhou JS, Hu JG, and Lu HZ. 2017. Transcriptome profile of rat genes in injured spinal cord at different stages by RNA-sequencing. *BMC Genomics* 18:173. 10.1186/s12864-017-3532-x

Singh A, Tetreault L, Kalsi-Ryan S, Nouri A, and Fehlings MG. 2014. Global prevalence and incidence of traumatic spinal cord injury. *Clin Epidemiol* 6:309-331. 10.2147/CLEP.S68889

Tisato V, Gallo S, Melloni E, Celeghini C, Passaro A, Zauli G, Secchiero P, Bergamini C, Trentini A, Bonaccorsi G, Valacchi G, Zuliani G, and Cervellati C. 2018. TRAIL and Ceruloplasmin Inverse Correlation as a Representative Crosstalk between Inflammation and Oxidative Stress. *Mediators Inflamm* 2018:9629537. 10.1155/2018/9629537

Tollner K, Brandt C, Romermann K, and Loscher W. 2015. The organic anion transport inhibitor probenecid increases brain concentrations of the NKCC1 inhibitor bumetanide. *Eur J Pharmacol* 746:167-173. 10.1016/j.ejphar.2014.11.019

Tran AP, Warren PM, and Silver J. 2018. The Biology of Regeneration Failure and Success After Spinal Cord Injury. *Physiol Rev* 98:881-917. 10.1152/physrev.00017.2017

Vergadi E, Ieronymaki E, Lyroni K, Vaporidi K, and Tsatsanis C. 2017. Akt Signaling Pathway in Macrophage Activation and M1/M2 Polarization. *J Immunol* 198:1006-1014. 10.4049/jimmunol.1601515

Wang JG, Williams JC, Davis BK, Jacobson K, Doerschuk CM, Ting JP, and Mackman N. 2011. Monocytic microparticles activate endothelial cells in an IL-1beta-dependent manner. *Blood* 118:2366-2374. 10.1182/blood-2011-01-330878

Wei R, Wang J, Xu Y, Yin B, He F, Du Y, Peng G, and Luo B. 2015. Probenecid protects against cerebral ischemia/reperfusion injury by inhibiting lysosomal and inflammatory damage in rats. *Neuroscience* 301:168-177. 10.1016/j.neuroscience.2015.05.070

Xiong XX, Gu LJ, Shen J, Kang XH, Zheng YY, Yue SB, and Zhu SM. 2014. Probenecid protects against transient focal cerebral ischemic injury by inhibiting HMGB1 release and

attenuating AQP4 expression in mice. *Neurochem Res* 39:216-224. 10.1007/s11064-013-1212-z

Yue B. 2014. Biology of the extracellular matrix: an overview. *J Glaucoma* 23:S20-23. 10.1097/IJG.0000000000000108

Zhang F, Ru N, Shang ZH, Chen JF, Yan C, Li Y, and Liang J. 2017. Daidzein ameliorates spinal cord ischemia/reperfusion injury-induced neurological function deficits in Sprague-Dawley rats through PI3K/Akt signaling pathway. *Exp Ther Med* 14:4878-4886. 10.3892/etm.2017.5166

Zhang Y, Yeh J, Richardson PM, and Bo X. 2008. Cell adhesion molecules of the immunoglobulin superfamily in axonal regeneration and neural repair. *Restor Neurol Neurosci* 26:81-96.

Zhou J, Xiong Q, Chen H, Yang C, and Fan Y. 2017. Identification of the Spinal Expression Profile of Non-coding RNAs Involved in Neuropathic Pain Following Spared Nerve Injury by Sequence Analysis. *Front Mol Neurosci* 10:91. 10.3389/fnmol.2017.00091Zhu Z, Wang D, Jiao W, Chen G, Cao Y, Zhang Q, and Wang J. 2017. Bioinformatics analyses of pathways and gene predictions in IL-1alpha and IL-1beta knockout mice with spinal cord injury. *Acta Histochem* 119:663-670. 10.1016/j.acthis.2017.07.007

Figures

Figure 1 PCA analysis

PCA analysis was performed using three principal components (PC1, 2, and 3) to demonstrate the source of variance (n=3).

Figure 2 Volcano map of DEGs

Red, green and blue dots represent significantly upregulated, downregulated and no changed gene expressions, respectively. (A) SCI_C vs Sham; (B) SCI_P vs SCI_C.

Figure 3 RT-qPCR verification of DEGs characterized by RNA-Seq

A: The longitudinal coordinates in RNA-Seq were the mRNA expression level (read counts, n = 3). B: The longitudinal coordinates in RT-qPCR were the mRNA expression level calculated using the $^{\Delta\Delta}$Ct method and expressed relative to the value in the sham group (designated as 1). All data were calculated with mean ± standard deviation (n = 6, which included 3 independent samples and the 3 same samples used for the RNA-seq analysis). **P < 0.01 (ANOVA).

Figure 4 Hierarchical cluster analysis of DEGs

The DEGs in different groups were analyzed using FPKM hierarchical cluster analysis. The read count numbers of FPKM were converted by RSEM software. DEGs were classified into different expression cluster by hierarchical clustering. The colour scheme (red to blue) represents the up to down of the gene expression. sham: sham group; SCI_C: SCI (solvent control) group; SCI_P: SCI (probenecid) group.

Figure 5 Subcluster analysis of DEGs

The subclusters of DEGs which have similar expression trends were further analyzed. The log2 (ratios) in SCI_C group ≥ 1 or ≤ -1 was used as a cut-off. Based on log2 (ratios) of the gene expression level relative to that of sham group, the log2 (ratios) of all gene expression levels in sham group were zero. A and B: the two subclusters which were strongly upregulated following SCI, and then downregulated upon probenecid treatment. C and D: the two subclusters which were strongly downregulated following SCI, and then upregulated upon probenecid treatment.

Figure 6 GO enrichment analysis of DEGs

DEGs were implemented by the GOseq R package, in which gene length bias was corrected. GO terms with corrected P value ≤ 0.05 were considered significantly enriched by DEGs. The asterisk (*) represent significant enrichment terms (P ≤ 0.05). A: GO analysis of upregulated DEGs in SCI_C vs sham group; B: GO analysis of downregulated DEGs in SCI_C vs sham group; C: GO analysis of downregulated DEGs in SCI_P vs SCI_C group.

Figure 7 KEGG enrichment analyses of DEGs

KOBAS software was used to test the statistical enrichment of DEGs in KEGG pathways. In this figure, KEGG enrichment is measured by Rich factor, Qvalue and the number of genes enriched in the related pathway. Rich factor refers to the ratio of the number of differentiated genes (sample number) enriched in the pathway to the number of annotated genes (background number). The larger the Rich factor, the greater the degree of enrichment. Qvalue is the Pvalue after multiple hypothesis test correction. The range of Qvalue is between 0 and 1. The closer the Qvalue is to 0, the more significant the enrichment is. The KEGG pathways were shown in A: upregulated DEGs (SCI_C vs sham); B: downregulated DEGs; C: upregulated DEGs (SCI_P vs SCP_C); D: downregulated DEGs (SCI_C vs sham).

Tables

Table 1 PCR primers used in the study
Table 2 Summary of sequence assembly after Illumina sequencing

Supplementary materials

Table S1 DEGs of different groups
Table S2 GO enrichment analysis of SCI_C vs sham group
Table S3 GO enrichment analysis of SCI_P vs SCI_C group
Table S4 KEGG analysis of SCI_C vs sham group
Table S5 KEGG analysis of SCI_P vs SCI_C group

Figure 1

Figure 1 PCA analysis

PCA analysis was performed using three principal components (PC1, 2, and 3) to demonstrate the source of variance (n=3).

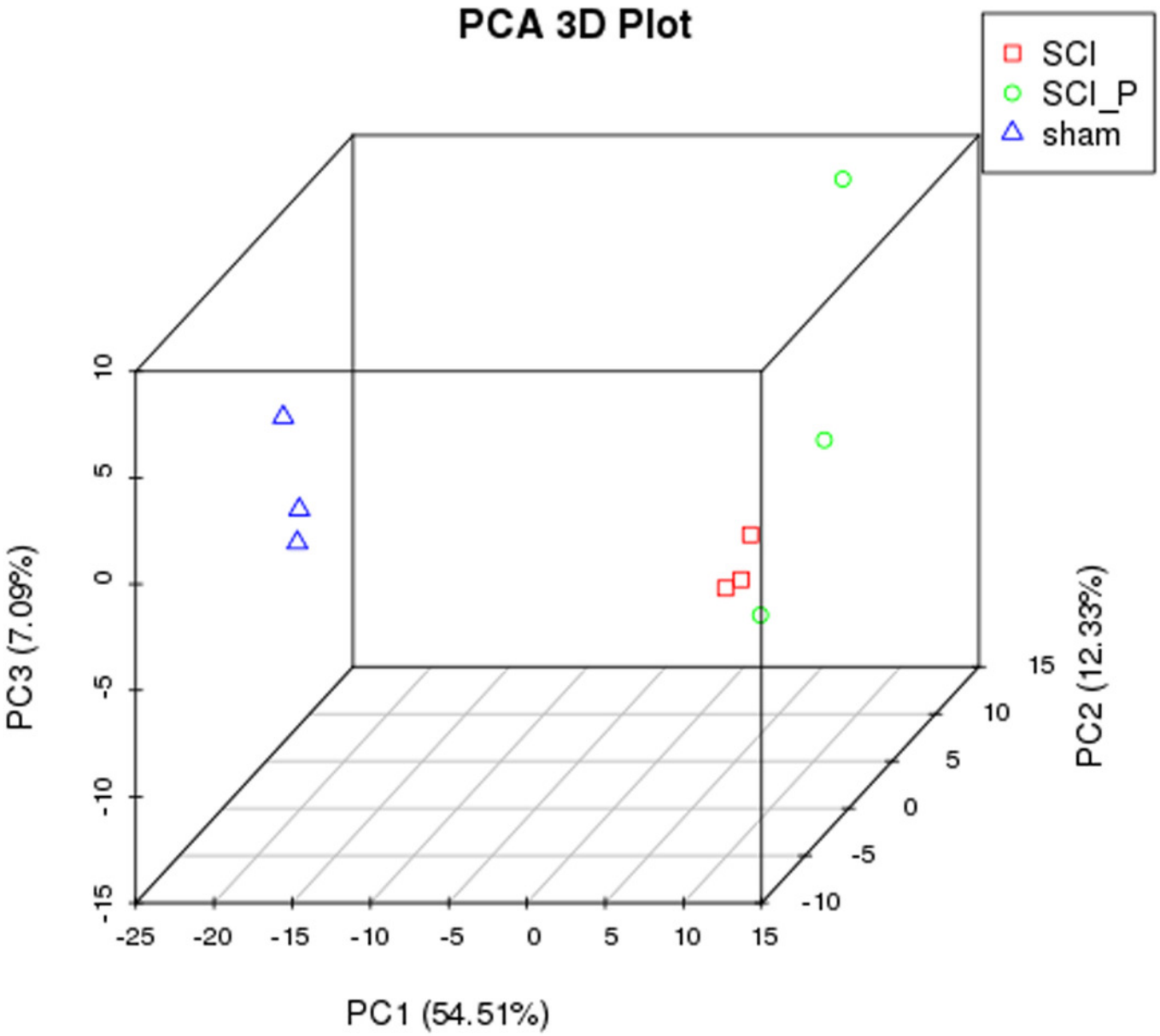

Figure 2

Figure 2 Volcano map of DEGs

Red, green and blue dots represent significantly upregulated, downregulated and no changed gene expressions, respectively. (A) SCI_C vs Sham; (B) SCI_P vs SCI_C.

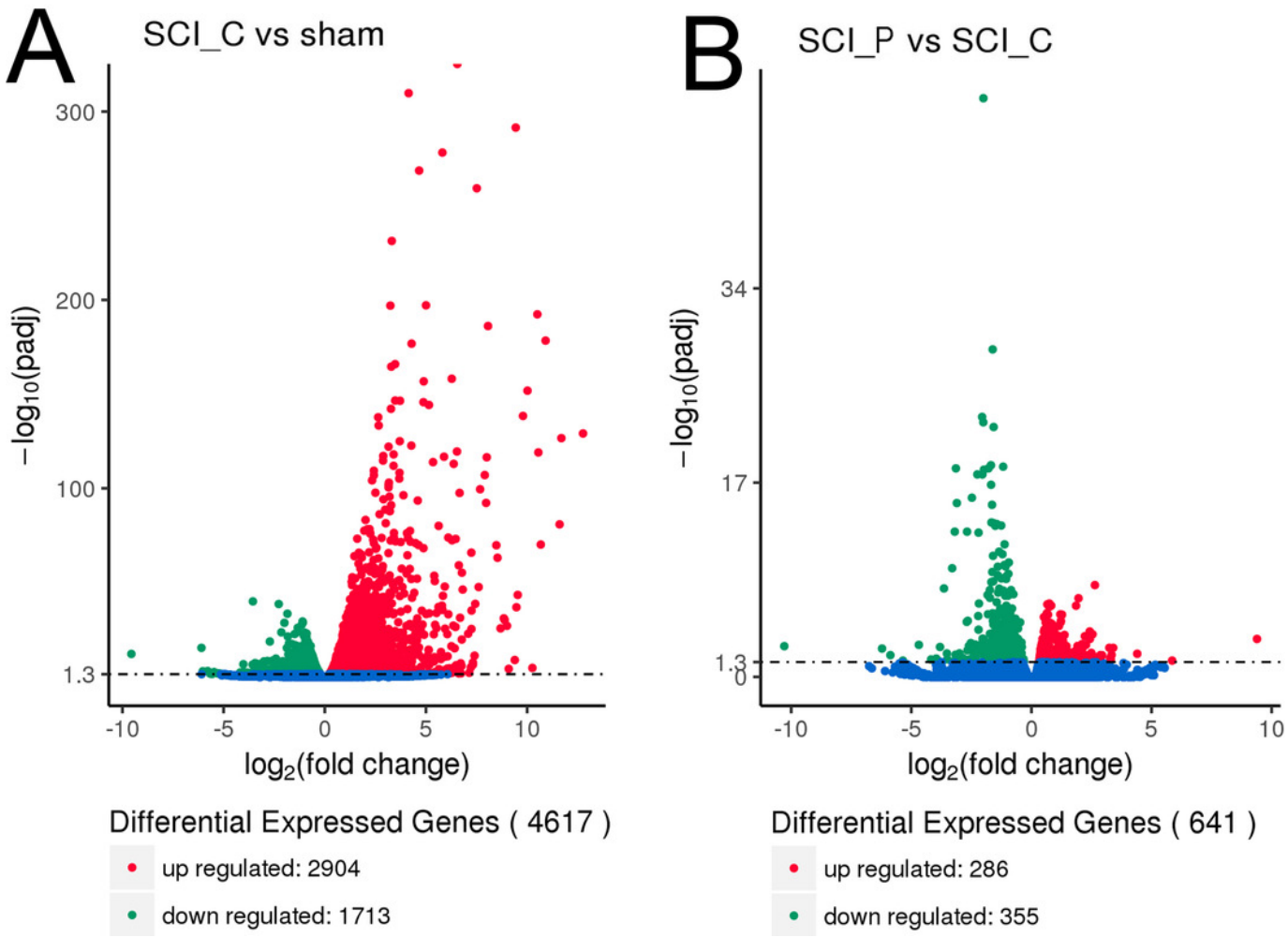

Figure 3

Figure 3 RT-qPCR verification of DEGs characterized by RNA-Seq

A: The longitudinal coordinates in RNA-Seq were the mRNA expression level (read counts, n = 3). B: The longitudinal coordinates in RT-qPCR were the mRNA expression level calculated using the $^{\Delta\Delta}$Ct method and expressed relative to the value in the sham group (designated as 1). All data were calculated with mean ± standard deviation (n = 6, which included 3 independent samples and the 3 same samples used for the RNA-seq analysis). **P < 0.01 (ANOVA).

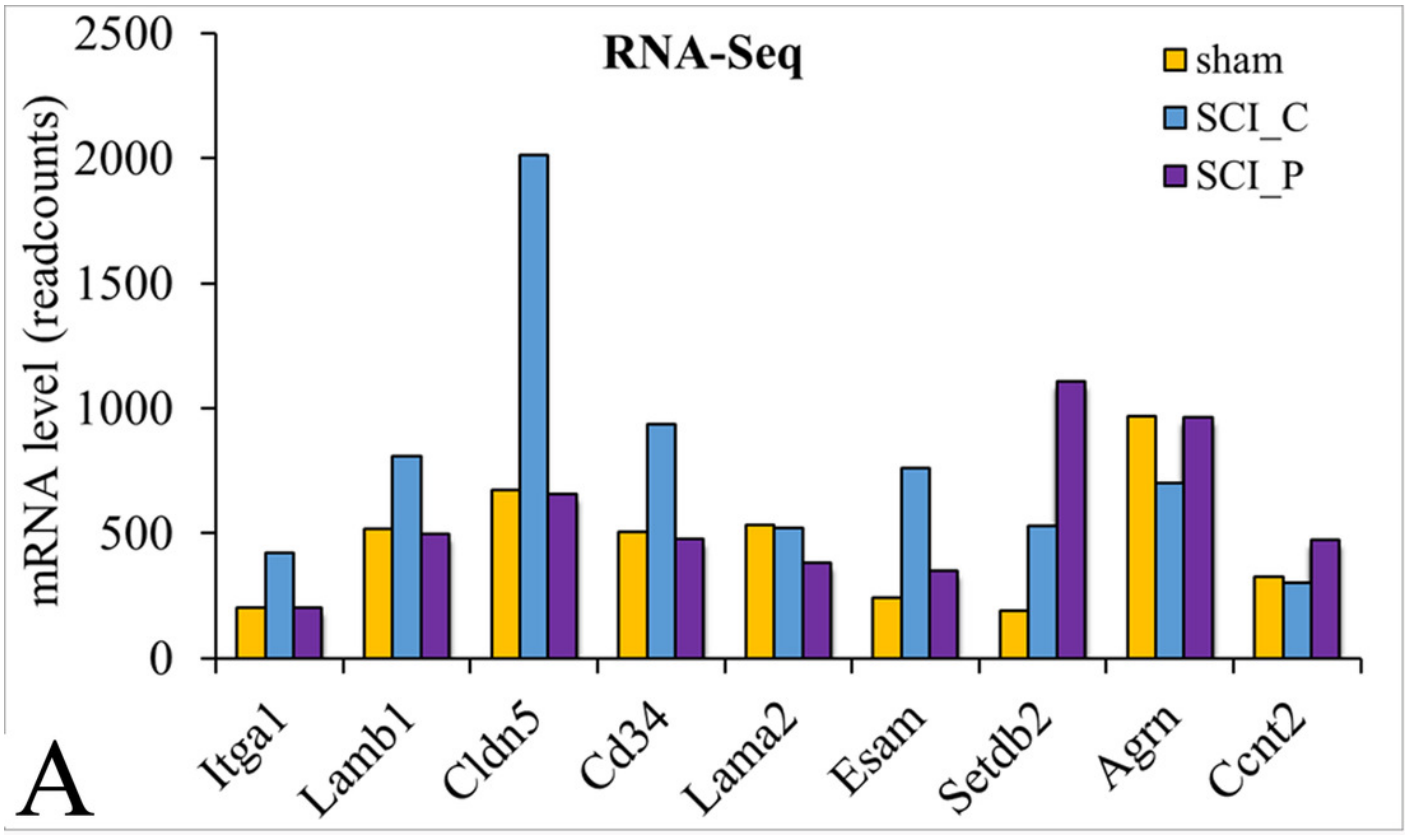
RNA-Seq
sham
SCI_C
SCI_P
mRNA level (readcounts)
2500
2000
1500
1000
500
0
Itga1
Lamb1
Cldn5
Cd34
Lama2
Esam
Setdb2
Agrn
Ccnt2
A

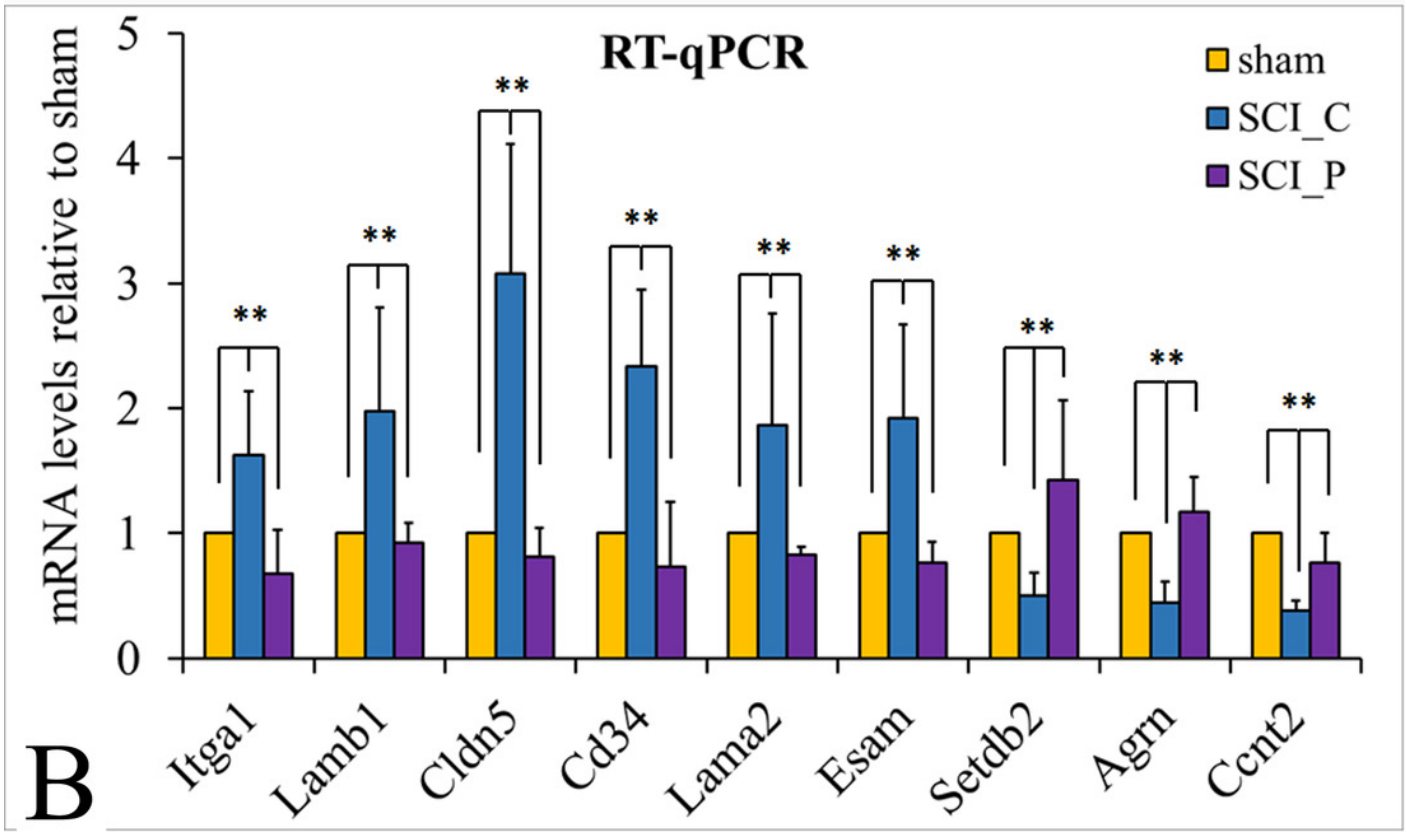
RT-qPCR
sham
SCI_C
SCI_P
mRNA levels relative to sham
5
4
3
2
1
0
**
Itga1
Lamb1
Cldn5
Cd34
Lama2
Esam
Setdb2
Agrn
Ccnt2
B

Figure 4

Figure 4 Hierarchical cluster analysis of DEGs

The DEGs in different groups were analyzed using FPKM hierarchical cluster analysis. The read count numbers of FPKM were converted by RSEM software. DEGs were classified into different expression cluster by hierarchical clustering. The colour scheme (red to blue) represents the up to down of the gene expression. sham: sham group; SCI_C: SCI (solvent control) group; SCI_P: SCI (probenecid) group.

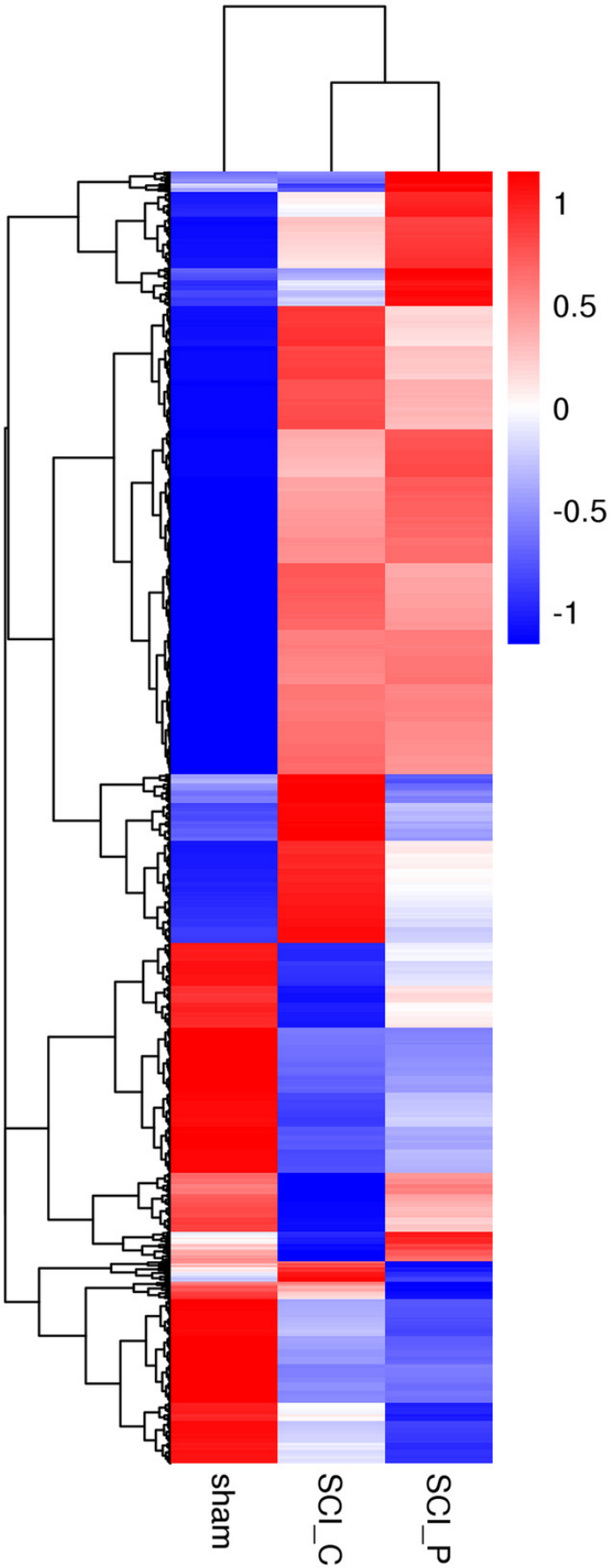
1
0.5
0
-0.5
-1
sham
SCI_C
SCI_P

Figure 5

Figure 5 Subcluster analysis of DEGs

The subclusters of DEGs which have similar expression trends were further analyzed. The log2 (ratios) in SCI_C group ≥ 1 or ≤ -1 was used as a cut-off. Based on log2 (ratios) of the gene expression level relative to that of sham group, the log2 (ratios) of all gene expression levels in sham group were zero. A and B: the two subclusters which were strongly upregulated following SCI, and then downregulated upon probenecid treatment. C and D: the two subclusters which were strongly downregulated following SCI, and then upregulated upon probenecid treatment.

A

Name	sham	SCI_C	SCI_P
Rgs16	0	1.78	1.07
Col4a1	0	1.7	0.9
Apobec3	0	1.66	1.29
Syk	0	1.65	0.89
Akr1b8	0	1.64	1.18
Ifi35	0	1.62	1.21
Thbs4	0	1.61	1.2
Esam	0	1.61	0.49
Pstpip2	0	1.59	0.58
Sdc1	0	1.58	1.05
Gda	0	1.58	0.85
A2m	0	1.57	1.42
Dok2	0	1.57	0.66
Nupr1	0	1.57	0.85
Aoc3	0	1.57	-0.41
Zfp429	0	1.54	0.65
Loxl4	0	1.53	1.05
Capg	0	1.52	0.9
Tnfrsf11b	0	1.52	1.37
Timeless	0	1.51	1.09
Plek	0	1.51	0.96
Naip2	0	1.51	1.22
Arhgef5	0	1.49	0.59
Slc1a5	0	1.48	0.68
Plekhg2	0	1.48	0.83
Anxa2	0	1.47	1.05
Cyp1b1	0	1.47	0.85
Tbx3	0	1.46	0.29
Tmem154	0	1.45	1
Emp3	0	1.44	1.12
Ptprc	0	1.43	0.57
Ets1	0	1.42	0.68
Mgp	0	1.41	0.28
Il33	0	1.41	0.85
Acat3	0	1.41	0.98
Anxa3	0	1.4	0.97
Cd52	0	1.4	0.22
Ltbr	0	1.4	1.06
Gjc1	0	1.4	0.87
Igfbp7	0	1.39	0.47
Stom	0	1.39	0.91
Gpr182	0	1.39	0.46
Hmga2	0	1.39	0.81
Steap3	0	1.39	0.73
Ncf2	0	1.37	0.96
Plp2	0	1.37	0.77
Phf11d	0	1.37	1.09
Nos3	0	1.35	0.06
Hspa4l	0	1.35	0.79
Adam12	0	1.34	0.82
Tgfb1	0	1.34	0.57
Rdh12	0	1.33	0.66
Marveld2	0	1.33	0.91
Alox5ap	0	1.3	0.03
Ap1s3	0	1.29	1.03
Ampd1	0	1.29	-1.8
Itgb2	0	1.29	0.33
Ip6k3	0	1.28	1.04
Snx20	0	1.28	0.5
Flt4	0	1.27	0.31
Spi1	0	1.26	0.71
Fblim1	0	1.24	0.81
Filip1l	0	1.24	0.41
Was	0	1.22	0.99
Arhgap30	0	1.22	0.83
Slc39a1	0	1.21	0.96
Rin3	0	1.21	0.39
Emilin1	0	1.21	0.7
Erg	0	1.21	0.13
Entpd1	0	1.2	0.46
Notch4	0	1.2	0.43
Pear1	0	1.19	0.08
Hcls1	0	1.18	0.76
Nfam1	0	1.17	0.49
Parp10	0	1.16	0.81
Dkk2	0	1.15	-0.12
Zfp217	0	1.15	0.79
Iqgap1	0	1.14	0.64
Ier5l	0	1.14	0.71
Msn	0	1.13	0.73
Icam2	0	1.13	0.1
Itgam	0	1.13	0.57
Plekha4	0	1.12	-0.33
Irf8	0	1.12	0.25
C1ra	0	1.12	0.47
Atp10a	0	1.11	0.51
Slc25a24	0	1.1	0.74
Cd33	0	1.1	0.68
Tarm1	0	1.1	0.24
Kcnj8	0	1.1	0.38
Hmgcs2	0	1.09	-0.61
Trim56	0	1.07	0.73
Sp100	0	1.07	-0.1
Trpm6	0	1.07	0.39
Erbb2	0	1.06	0.45
Id3	0	1.06	0.51
Tbxa2r	0	1.05	-0.96
Foxq1	0	1.05	-0.44
Myo1c	0	1.05	0.6
Arhgdib	0	1.05	0.34
Fbln2	0	1.04	0.3
Apobr	0	1.04	0.37
Hk3	0	1.04	0.5
Fxyd3	0	1.02	-0.32
Cybb	0	1	-0.71
Ptrh1	0	1	0.33

B

Name	sham	SCI_C	SCI_P
Sox7	0	1.49	0.65
S100a6	0	1.48	1.34
Tnfrsf10b	0	1.48	0.96
Lyn	0	1.42	1.2
Trib3	0	1.4	1.03
Tpm4	0	1.39	1.02
Rac2	0	1.36	1.06
Tec	0	1.3	1.15
Wwtr1	0	1.29	1.03
Slc5a3	0	1.27	1.09
Yap1	0	1.27	0.98
Fcer1g	0	1.26	1.06
Ecm1	0	1.25	0.61
Ptpn12	0	1.25	1.08
Itpripl1	0	1.23	0.86
Gpd1	0	1.22	1.1
Id1	0	1.2	0.62
S100a10	0	1.19	1
Met	0	1.18	1.01
Wisp1	0	1.18	1.01
Slc2a1	0	1.18	0.72
Twist1	0	1.17	0.26
Mb21d1	0	1.17	0.88
Ddx58	0	1.16	1.02
Layn	0	1.16	1.12
Tmem37	0	1.16	0.51
Cavin1	0	1.15	0.65
Ldha	0	1.14	0.74
Lrrn4cl	0	1.14	0.28
Cyba	0	1.14	0.56
Adipor2	0	1.13	0.97
Myh9	0	1.12	0.79
Casp12	0	1.12	0.99
Vsig2	0	1.11	0.4
Fhl3	0	1.11	0.9
Rhoc	0	1.11	0.91
Rbpms	0	1.1	0.29
Lrrc8a	0	1.1	0.98
Xbp1	0	1.1	0.64
Susd6	0	1.09	0.98
Cdc42se1	0	1.07	1
Myo1g	0	1.07	0.69
Rph3al	0	1.07	0.72
Nfya	0	1.06	-0.11
Cflar	0	1.05	0.67
Psmb8	0	1.04	0.7
Vgf	0	1.04	0.69
Dll4	0	1.03	0.42
Tnfaip8l1	0	1.03	0.84
Ncf1	0	1.03	0.77
Gypc	0	1.02	0.74
Cd63	0	1.02	0.86
Psd4	0	1.01	0.72
Tspo	0	1	0.56

C

Name	sham	SCI_C	SCI_P
Snrnp40	0	-2.24	-1.44
Ranbp3l	0	-2.18	-1.9
Wdr49	0	-2.11	-0.93
Ly6g6f	0	-1.86	-1.72
Lrrc43	0	-1.68	-1.49
Gpr17	0	-1.52	-1.18
Gli1	0	-1.44	-1.24
Mob3b	0	-1.32	-1.24
Hoxd1	0	-1.31	-0.87
Rgs22	0	-1.28	-0.84
Gdf7	0	-1.27	-0.99
Cep72	0	-1.2	-0.75
Vwa3a	0	-1.2	-0.86
Dynlrb2	0	-1.2	-0.98
Serpinb1	0	-1.19	-1
Opn4	0	-1.17	-0.78
Cd180	0	-1.17	-0.85
Crb1	0	-1.12	-0.37
Msx1	0	-1.12	-0.98
Fgfr2	0	-1.11	-0.87
Dlec1	0	-1.1	-0.61
Lrrc23	0	-1.08	-0.78
Myh6	0	-1.06	-0.78
Pls1	0	-1.05	-0.73
Neil2	0	-1.05	-0.29
Calr4	0	-1.04	-0.79
Efs	0	-1.03	-0.87
Adamts6	0	-1.03	-0.67
Hhip	0	-1.02	-0.84

D

Name	sham	SCI_C	SCI_P
Gm6408	0	-4.63	-1.3
Slc26a9	0	-3.9	0.009
Olfr1393	0	-3.4	-0.68
Lrrc27	0	-3.04	-1.97
Sis	0	-2.82	-1.26
Vmn1r4	0	-2.65	0.032
Ctcfl	0	-2.54	0.263
Klf14	0	-2.47	-0.77
Esco2	0	-2.45	-1.34
Olfr545	0	-2.38	0.12
Gm47283	0	-2.31	-0.26
Gm40460	0	-2.31	-0.71
Wdr86	0	-2.28	-0.83
Esrp1	0	-2.21	-0.51
E2f8	0	-2.2	-1.93
Oard1	0	-2.04	-2.05
Emilin3	0	-2	1.398
Tulp1	0	-1.91	-0.52
Ccdc153	0	-1.9	-1.44
Lmntd1	0	-1.89	-1.28
Iqca	0	-1.89	-1
Pitx1	0	-1.88	-1.59
Tmem212	0	-1.87	-1.08
Mc5r	0	-1.85	-1.28
Smim5	0	-1.84	-1.27
D6Ertd527e	0	-1.84	0.325
Ccdc146	0	-1.81	-0.66
Col6a6	0	-1.81	-0.06
Nme9	0	-1.74	-1.43
Fam166b	0	-1.72	-1.38
Ildr1	0	-1.71	-0.99
Adgrf4	0	-1.67	-0.18
Lgr6	0	-1.66	-1.49
BC024139	0	-1.65	-1.22
C1qtnf3	0	-1.62	-1.38
Acp4	0	-1.61	0.21
Dnah8	0	-1.6	-0.66
Accsl	0	-1.6	1.376
Stpg1	0	-1.59	-1.08
Dnah11	0	-1.57	-0.7
Ninj2	0	-1.57	-1.23
Slc27a5	0	-1.55	-0.08
Tex35	0	-1.54	0.708
Rad9a	0	-1.53	1.005
Fscn2	0	-1.52	1.093
Ttc16	0	-1.52	-1.01
Morn5	0	-1.47	-0.28
Frmpd2	0	-1.47	-0.64
Col24a1	0	-1.46	-0.24
Lrit3	0	-1.43	0.398
Atp10b	0	-1.43	-1.11
Sctr	0	-1.4	-0.55
Cfap70	0	-1.38	-0.41
Vwa3b	0	-1.38	-0.59
Cdhr3	0	-1.37	-0.64
Siglech	0	-1.35	-1
Angptl1	0	-1.34	-1.49
Kctd14	0	-1.33	-0.79
Abcg5	0	-1.33	1.534
Ing4	0	-1.31	-0.23
Gm10775	0	-1.29	-0.07
Mpp4	0	-1.29	0.129
Mcm10	0	-1.27	0.212
Neu4	0	-1.26	-1.14
Aipl1	0	-1.25	1.265
Olfml1	0	-1.24	-1.02
Cubn	0	-1.24	-0.12
Barx2	0	-1.23	-0.31
Slc34a3	0	-1.19	-0.83
Tmem210	0	-1.17	-0
Adamts19	0	-1.16	-0.43
Cavin4	0	-1.16	-0.7
Col11a1	0	-1.13	-0.26
H2-Bl	0	-1.13	-0.45
Nudt8	0	-1.12	-0.32
Chrd	0	-1.12	-0.41
Cfap44	0	-1.12	-0.1
Casc1	0	-1.1	-0.24
Gipr	0	-1.1	-0.65
Ccdc162	0	-1.09	-0.56
Tnfrsf4	0	-1.09	-0.41
Pcsk4	0	-1.08	-0.41
Fxyd2	0	-1.05	-0.57
Kif20b	0	-1.05	-0.58
Pld6	0	-1.04	-0.44
Entpd4b	0	-1.03	-0
Col11a2	0	-1.03	-0.47
Riiad1	0	-1.02	-0.43
Ager	0	-1.01	-0.17
Catsperd	0	-1.01	-0.26
Rxfp1	0	-1.01	-0.48
Smc1b	0	-1	0.496
F2rl3	0	-1	-0.2
Poln	0	-1	-0.24

Figure 6

Figure 6 GO enrichment analysis of DEGs

DEGs were implemented by the GOseq R package, in which gene length bias was corrected. GO terms with corrected P value ≤ 0.05 were considered significantly enriched by DEGs. The asterisk (*) represent significant enrichment terms (P ≤ 0.05). A: GO analysis of upregulated DEGs in SCI_C vs sham group; B: GO analysis of downregulated DEGs in SCI_C vs sham group; C: GO analysis of downregulated DEGs in SCI_P vs SCI_C group.

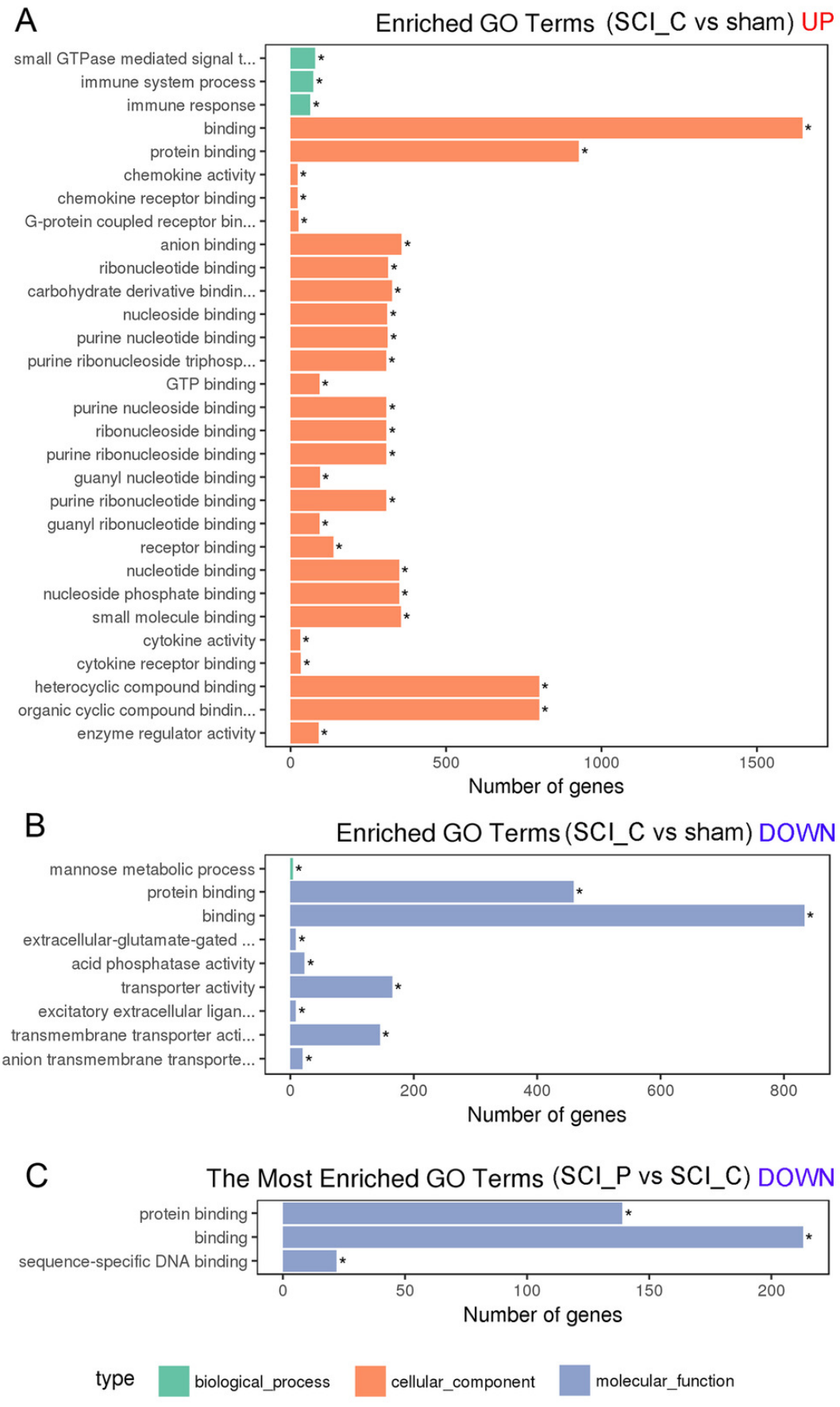
A
Enriched GO Terms (SCI_C vs sham) UP
small GTPase mediated signal t...
immune system process
immune response
binding
protein binding
chemokine activity
chemokine receptor binding
G-protein coupled receptor bin...
anion binding
ribonucleotide binding
carbohydrate derivative bindin...
nucleoside binding
purine nucleotide binding
purine ribonucleoside triphosp...
GTP binding
purine nucleoside binding
ribonucleoside binding
purine ribonucleoside binding
guanyl nucleotide binding
purine ribonucleotide binding
guanyl ribonucleotide binding
receptor binding
nucleotide binding
nucleoside phosphate binding
small molecule binding
cytokine activity
cytokine receptor binding
heterocyclic compound binding
organic cyclic compound bindin...
enzyme regulator activity
0
500
1000
1500
Number of genes
B
Enriched GO Terms (SCI_C vs sham) DOWN
mannose metabolic process
protein binding
binding
extracellular-glutamate-gated ...
acid phosphatase activity
transporter activity
excitatory extracellular ligan...
transmembrane transporter acti...
anion transmembrane transporte...
0
200
400
600
800
Number of genes
C
The Most Enriched GO Terms (SCI_P vs SCI_C) DOWN
protein binding
binding
sequence-specific DNA binding
0
50
100
150
200
Number of genes
type
biological_process
cellular_component
molecular_function

Figure 7

Figure 7 KEGG enrichment analyses of DEGs

KOBAS software was used to test the statistical enrichment of DEGs in KEGG pathways. In this figure, KEGG enrichment is measured by Rich factor, Qvalue and the number of genes enriched in the related pathway. Rich factor refers to the ratio of the number of differentiated genes (sample number) enriched in the pathway to the number of annotated genes (background number). The larger the Rich factor, the greater the degree of enrichment. Qvalue is the Pvalue after multiple hypothesis test correction. The range of Qvalue is between 0 and 1. The closer the Qvalue is to 0, the more significant the enrichment is. The KEGG pathways were shown in A: upregulated DEGs (SCI_C vs sham); B: downregulated DEGs; C: upregulated DEGs (SCI_P vs SCP_C); D: downregulated DEGs (SCI_C vs sham).

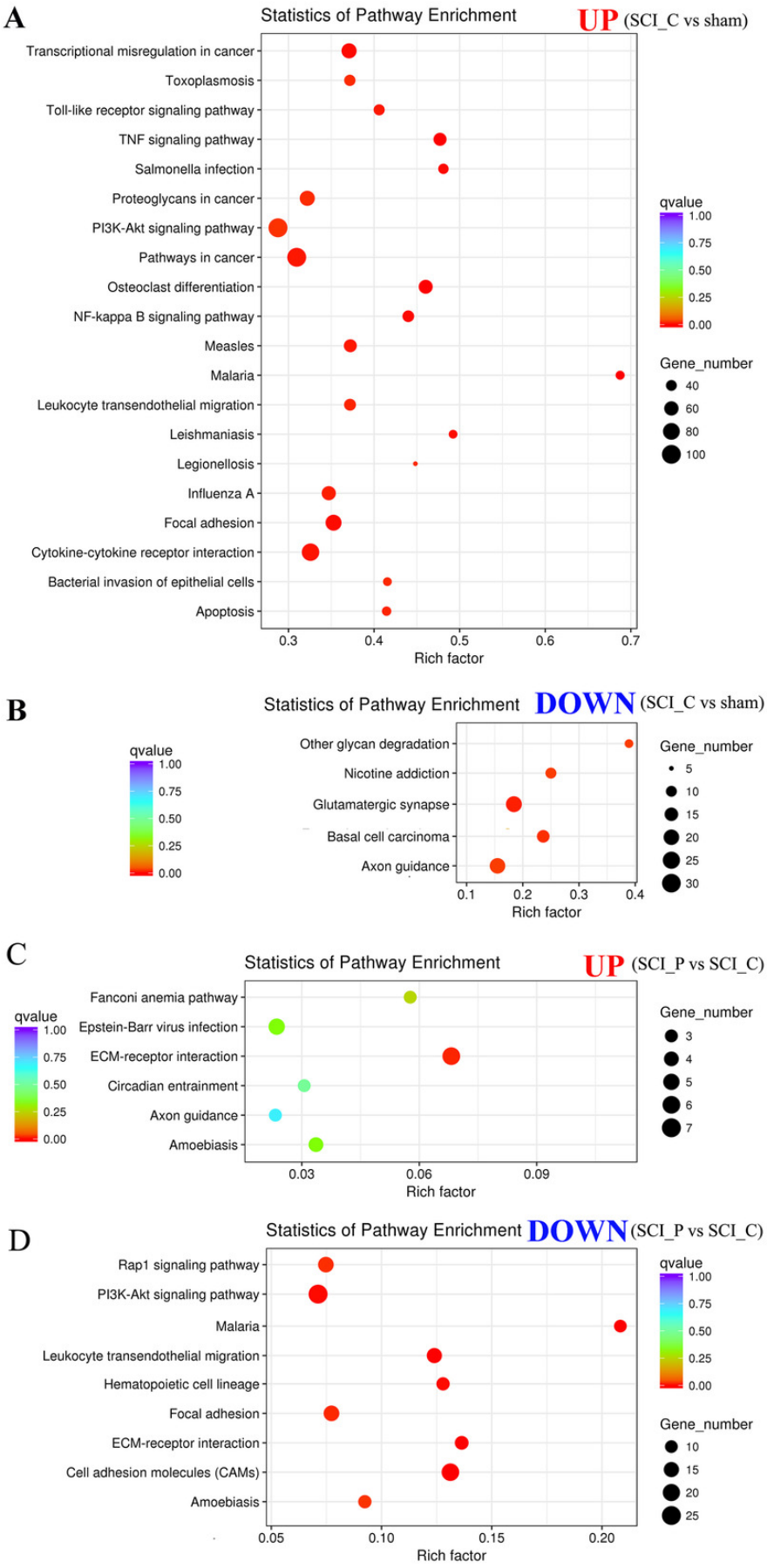
A
Statistics of Pathway Enrichment
UP (SCI_C vs sham)
Transcriptional misregulation in cancer
Toxoplasmosis
Toll-like receptor signaling pathway
TNF signaling pathway
Salmonella infection
Proteoglycans in cancer
PI3K-Akt signaling pathway
Pathways in cancer
Osteoclast differentiation
NF-kappa B signaling pathway
Measles
Malaria
Leukocyte transendothelial migration
Leishmaniasis
Legionellosis
Influenza A
Focal adhesion
Cytokine-cytokine receptor interaction
Bacterial invasion of epithelial cells
Apoptosis
0.3
0.4
0.5
0.6
0.7
Rich factor
qvalue
1.00
0.75
0.50
0.25
0.00
Gene_number
40
60
80
100
B
Statistics of Pathway Enrichment
DOWN (SCI_C vs sham)
Other glycan degradation
Nicotine addiction
Glutamatergic synapse
Basal cell carcinoma
Axon guidance
0.1
0.2
0.3
0.4
Rich factor
qvalue
1.00
0.75
0.50
0.25
0.00
Gene_number
5
10
15
20
25
30
C
Statistics of Pathway Enrichment
UP (SCI_P vs SCI_C)
Fanconi anemia pathway
Epstein-Barr virus infection
ECM-receptor interaction
Circadian entrainment
Axon guidance
Amoebiasis
0.03
0.06
0.09
Rich factor
qvalue
1.00
0.75
0.50
0.25
0.00
Gene_number
3
4
5
6
7
D
Statistics of Pathway Enrichment
DOWN (SCI_P vs SCI_C)
Rap1 signaling pathway
PI3K-Akt signaling pathway
Malaria
Leukocyte transendothelial migration
Hematopoietic cell lineage
Focal adhesion
ECM-receptor interaction
Cell adhesion molecules (CAMs)
Amoebiasis
0.05
0.10
0.15
0.20
Rich factor
qvalue
1.00
0.75
0.50
0.25
0.00
Gene_number
10
15
20
25

Table 1(on next page)

Table 1 PCR primersused in the study

1 **Table 1 Real-time PCR primers used in the study**

2

Gene	Forward primer 5' - 3'	Reverse primer 5' - 3'
Itga1	TCAGTGGAGAGCAGATCGGA	CCTCGTCTGATTCACAGCGT
lamb1	TGCCTTTTCTCCCCGCTACC	CCATGTCCAGTCCTCGCAGA
Cldn5	TTCTATGATCCGACGGTGCC	CTTGACCGGGAAGCTGAACT
CD34	ACCACAGACTTCCCCAACTG	CATATGGCTCGGTGGGTGAT
lama2	GCATTAGTGAGCCGCCCTAT	TCTTTCAGGTCTCGTGTGGC
Esam	AGACTCTGGGACTTACCGCT	GGTCACATTGGTCCCGACAT
Setdb2	CCACAAATGGAGATCATACACCT	GCAGTGGGGCTTCCTTTTTC
Agrn	CTCTGCCACTGGAACACAGA	GGAAAAGCAGCACCGCAAAG
Ccnt2	AGCAAGGATTTGGCACAGAC	CTCTAGGGTAACCGTGGGGT
beta-actin	AGAAGCTGTGCTATGTTGCTCTA	ACCCAAGAAGGAAGGCTGGAAAA

Table 2(on next page)

Table 2 Summary of sequence assembly after Illumina sequencing

Sham: Sham_1, Sham_2, Sham_3; SCI (solvent control): SCI_C1, SCI_C2, SCI_C3; SCI (probenecid): SCI_P1, SCI_P2, SCI_P3; Q20: The percentage of bases with a Phred value > 20; Q30: The percentage of bases with a Phred value > 30.

Table 2 Summary of sequence assembly after Illumina sequencing

Sample name	Raw reads	Clean reads	clean bases	Error rate (%)	Q20 (%)	Q30 (%)	GC content (%)
Sham_1	56509230	55796658	8.37G	0.03	97.73	93.95	51.23
Sham_2	48848744	48226002	7.23G	0.03	97.6	93.67	51.71
Sham_3	58228350	57459748	8.62G	0.03	97.67	93.78	51.42
SCI_C1	58862872	58126844	8.72G	0.03	97.88	94.31	51.39
SCI_C2	56980070	56166058	8.42G	0.03	97.74	94.03	51.42
SCI_C3	59804518	58798224	8.82G	0.03	97.63	93.74	51.02
SCI_P1	54853344	53996254	8.1G	0.03	97.72	93.91	50.93
SCI_P2	56322736	55540308	8.33G	0.03	97.87	94.27	50.94
SCI_P3	61037096	60037772	9.01G	0.03	97.71	93.89	50.92

Sham: Sham_1, Sham_2, Sham_3; SCI (solvent control): SCI_C1, SCI_C2, SCI_C3; SCI (probenecid): SCI_P1, SCI_P2, SCI_P3;

Q20: The percentage of bases with a Phred value > 20;

Q30: The percentage of bases with a Phred value > 30.